Poor-solvent polyelectrolytes

2003 J. Phys.: Condens. Matter 15 S205

(http://iopscience.iop.org/0953-8984/15/1/326)

INSTITUTE OF PHYSICS PUBLISHING JOURNAL OF PHYSICS: CONDENSED MATTER

J. Phys.: Condens. Matter **15** (2003) S205–S211 PII: S0953-8984(03)54837-8

Poor-solvent polyelectrolytes

C Holm[1], **H J Limbach and K Kremer**

Max-Planck-Institut für Polymerforschung, Ackermannweg 10, 55128 Mainz, Germany

E-mail: holm@mpip-mainz.mpg.de, limbach@mpip-mainz.mpg.de and kremer@mpip-mainz.mpg.de

Received 16 October 2002
Published 16 December 2002
Online at stacks.iop.org/JPhysCM/15/S205

Abstract

Using extensive molecular dynamics simulations we study the behaviour of polyelectrolytes (PEs) in poor solvents, explicitly taking the counterions into account. The resulting pearl-necklace structures are subject to strong conformational fluctuations. These lead to small signatures in the form factor and the force–extension relation, which is a severe obstacle to experimental observations. In addition, we study how the necklace collapses as a function of the Bjerrum length. Finally, we demonstrate that the position of the first peak in the inter-chain structure factor varies with the monomer density as $\approx\rho_m^{0.35}$ for all densities, which shows a pertinent different behaviour as compared to that of PE solutions in good solvent.

1. Introduction

Polyelectrolytes (PEs) are polymers which have the ability to dissociate charges in polar solvents, resulting in charged polymer chains (macroions) and mobile counterions. They represent a broad and interesting class of soft matter [1, 2] that are attracting increasing attention in the scientific community. In technical applications, PEs are used as viscosity modifiers, as precipitating agents, and as superabsorbers. A thorough understanding of charged soft matter has become of great interest also in biochemistry and molecular biology. This is due to the fact that virtually all proteins, as well as other biopolymers such as DNA, actin, and microtubules, are PEs.

Many PEs possess a hydrocarbon-based backbone for which water is a very poor solvent. Therefore, in aqueous solution, there is a competition between the solvent quality, the Coulombic interaction, and the entropic degrees of freedom. The conformation in these systems can under certain conditions assume pearl-necklace-like structures [3–5]. In earlier simulations [6–8] of these systems it was found that the polymer density can be used as a very simple parameter to separate different conformational regimes. Here we analyse in more detail the single-chain behaviour and the scaling of the peak in the inter-chain structure function.

[1] Author to whom any correspondence should be addressed.

2. Simulation model

Our PE model and molecular dynamics (MD) approach has been described in [6–8] and consists of a bead–spring chain of Lennard-Jones (LJ) particles. Chain monomers interact via a LJ interaction up to a distance $R_c = 2.5\,\sigma$ and experience an attraction with $\epsilon = 1.75\,k_BT$. The Θ point for this model is at $\epsilon = 0.34\,k_BT$ [6]. The counterions interact via a purely repulsive LJ interaction. For bonded monomers we add a FENE bond potential. Charged particles at separation r interact via the Coulomb energy $k_BT\ell_b q_i q_j/r$, with $q_i = 1$ (-1) for the charged chain monomers (counterions) and the Bjerrum length $\ell_b = e^2/(4\pi\epsilon_S\epsilon_0 k_BT)$ (e: unit charge; ϵ_0 and ϵ_S: permittivity of the vacuum and of the solvent). We simulated various systems with several chains in the central simulation box at various monomer densities ρ_m and different values of ℓ_b. Each chain consists of $N_m = 48, \ldots, 478$ monomers, with a charge fraction $f = 1/3$ to 1. The pressure p was found to be always positive, with the p–V diagram being convex at all densities; thus our simulations are stable, reach true thermal equilibrium, and reside in a one-phase region.

3. Single-chain properties

3.1. Fluctuations

With the help of a specially developed cluster algorithm [8] that automatically recognizes the number of pearls in a conformation, we have analysed all equilibrium conformations in our systems. We found a large coexistence regime of several pearl structures consisting of conformations with different numbers of pearls. Even a single chain shows over a course of time many transitions between different pearl structures; hence the different pearl states are not frozen or metastable. Also the position and size of the pearls and strings are constantly changing [8, 9]. We furthermore found that the lower the number of pearls, the stronger the attraction of the counterions to the pearls. The integrated ion distribution versus the chain distance displays an inflection point, which is a signal of counterion condensation [10]. In contrast to analytical theory predictions [11], the pearl structures are stable, even though there are counterions localized near and/or inside the pearls.

3.2. Approaching the collapsed state

When one starts in a necklace conformation and increases ℓ_b, the counterions will get attracted more and more towards the chain. Scaling theories have predicted that with the onset of condensation the necklace state should collapse at a first-order transition into the globular state [5, 11–13]. However, the 'onset' of condensation is not a sharp border, rather like within Poisson–Boltzmann theory one finds a smooth distribution of counterions which gets weighted closer to the macroion as the coupling is increased [10]. Accordingly, in the simulation we do not observe a collapse transition. The picture is qualitatively the same as for the good-solvent case [14]. At $\ell_b = 0$ the chain is in a collapsed conformation. On increasing ℓ_b the chain first extends up to a maximum, and then slowly shrinks back to a collapsed state. The non-monotonic behaviour of the extension is qualitatively the same as in the good-solvent case [14]; however, the decrease is faster and more pronounced here [6, 15]. There is also a subtle dependence on f. The scaling variable which determines R_E of the necklace is $f^2\ell_b$ at fixed N_m and ϵ [5]. In figure 1 we have shown snapshots of chains with the same value of $f^2\ell_b$, but different f. The chain extension is drastically different, and depends on the local interactions mediated by the counterions. This effect is obviously not captured by the scaling

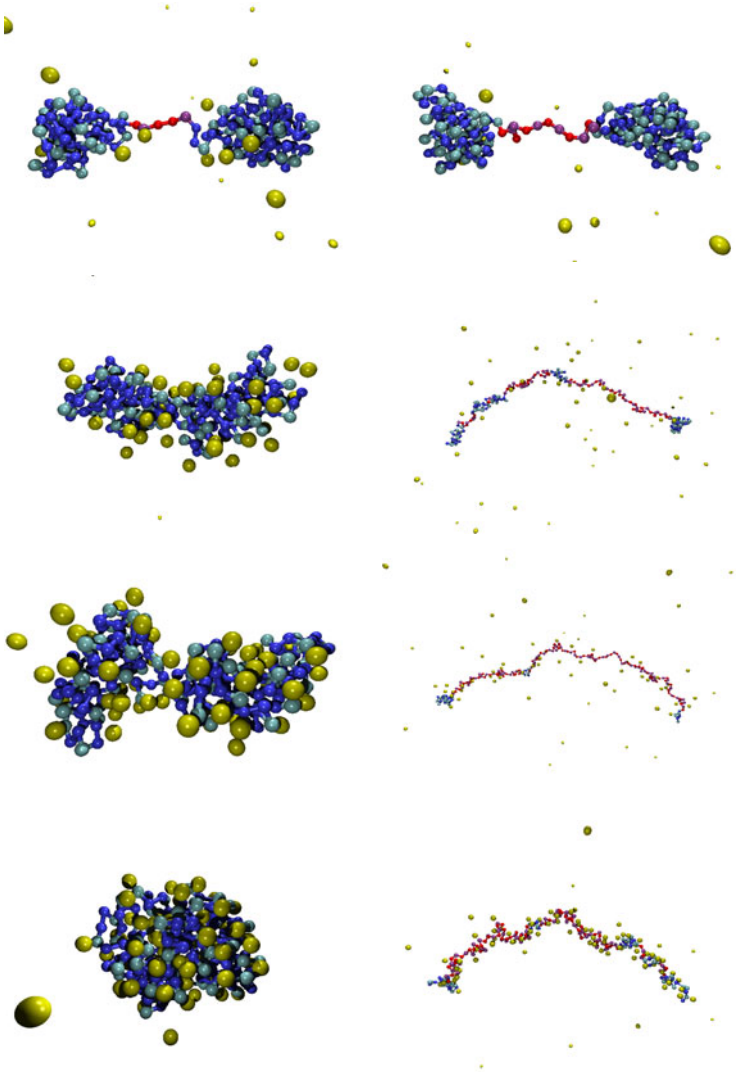

Figure 1. Snapshots for different values of the scaling variable $f^2\ell_b$. Left row: with $f = 1/3$; right row: with $f = 1/2$. From top to bottom, $f^2\ell_b$ has the values: 0.08 σ, 0.25 σ, 0.5 σ, 1.0 σ. System: eight chains with $N_m = 199$ monomers at $\rho_m = 5.0 \times 10^{-5}\ \sigma^{-3}$.

(This figure is in colour only in the electronic version)

ansatz. Note also that the conformations on the way to the collapsed globule are very much reminiscent of a cylindrical shape [12], since the strings become very short, and the pearls coalesce slowly on a one-dimensional string until they reach the globular state. The collapsed state is reached at roughly the same value of ℓ_b, which is reminiscent of the critical point of a Coulomb fluid.

3.3. The form factor

To see what could be observed in a scattering experiment we computed the spherically averaged form factor $S_1(q)$ of a single chain, shown in figure 2.

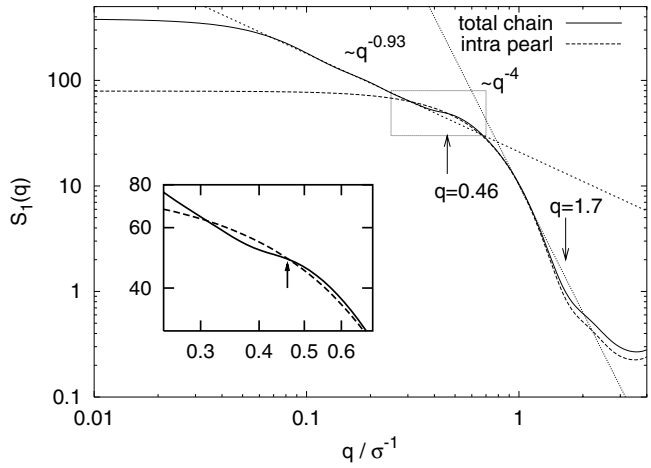

Figure 2. The spherically averaged form factor $S_1(q)$. Shown are the single-chain form factor (solid curve), together with the part of the form factor coming from the intra-pearl scattering (dashed curve). The dotted and short-dashed fits show the elongated chain part and the Porod scattering part (globular conformation). System: seven chains with 382 monomers, $f = 1/3$, $\ell_b = 1.5\,\sigma$, $\rho_m = 1.0 \times 10^{-5}\,\sigma^{-3}$.

In the range $1 < q\sigma < 2$ we note a sharp decrease in S_1, which comes from the scattering from the pearls, because it shows the typical Porod scattering of $S_1(q) \simeq q^{-4}$. The kink at $q\sigma \approx 1.66$ appears at the position expected from the pearl size, but is broadly smeared out due to large size fluctuations. The shoulder which can be seen at $q\sigma \approx 0.5$ does not come from the intra-pearl scattering but is due to the scattering of neighbouring pearls along the chain (inter-pearl contribution), which have a mean separation of $\langle r_{PP} \rangle = 13.3\,\sigma$. It is also smeared out due to the large distribution of inter-pearl distances. We conclude that the signatures of the pearl necklaces are already weak for monodisperse samples. A possible improvement could be achieved for chains of very large molecular weights and only few pearls, which could lead to stable and large signatures.

3.4. Force–extension relation

Next we performed simulations of stretching a single chain consisting of $N_m = 256$ charged monomers ($f = 1$) in the infinite-dilution limit; there are no counterions present. This is nowadays a standard technique performed with atomic-force microscopes (AFM) on single molecules. The LJ parameter was set to $\epsilon = 1.75\,k_BT$, and the Bjerrum length was set at $l_B = 0.08\,\sigma$; the chain is only weakly charged and close to the ones considered in the scaling approach [13, 16]. Technically we fix a certain end-to-end distance and measure the force acting on the end-monomers. In the unstretched state ($R_E = 21\,\sigma$) the system is in a two-pearl configuration. The first remarkable observation is that the two-pearl state evolves into a three-pearl state under extension, which was predicted by scaling [16], but is counter-intuitive from simple arguments. This is a result of the electrostatic inter-pearl interactions [8]. At each separation the chain was equilibrated and sampled over a long time in equilibrium, and the resulting force on the end-monomers was measured, yielding a continuous curve; see figure 3. Only when we perform averaging separately over the three-pearl and two-pearl states do we recognize a sawtooth pattern in the force, as predicted by scaling theories. In equilibrium one would expect a plateau for a true first-order transition, and the upper and lower parts would

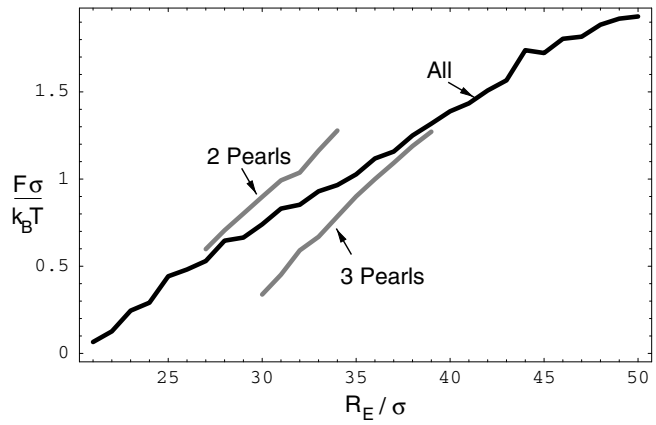

Figure 3. The force–extension relation for a transition from two to three pearls. Shown are the averages over all conformations (solid black), over only two-pearl configurations (top curve), and over only three-pearl configurations (bottom curve).

correspond to metastable superheated and supercooled states. Again, due to the large chain fluctuation and coexistence regime, all non-trivial signatures in the force–extension relation are basically washed out in equilibrium. Looking at the distribution of the hydrodynamic radius R_H for various end-to-end distances R_E, one can observe a clear bimodal distribution, showing that the transition between different pearl states is of first order. This can be seen particularly well in R_H, because it is simply related to the order parameter of the transition [17].

4. Scaling of the correlation length ξ

The overall scattering function $S(q)$ of the solution contains additional experimental information. We analyse here the inter-chain scattering $S_{IC} = S/S_1$, using again strongly charged PEs as in section 2. For good-solvent PEs, experiments [18], theory [19], and simulations [14] find a pronounced first peak of S_{IC} at $q^* = (2\pi)/\xi$, where ξ is the correlation length. The position varies as $q^* \propto \rho_m^{1/3}$ in the very dilute regime and crosses over to a $\rho_m^{1/2}$-regime at higher concentrations. In figure 4 we have plotted the density dependence of q^* in poor solvent for different chain lengths. Within the error bars we find that for poor-solvent chains, q^* scales proportionally to $\rho_m^{0.35\pm0.04}$ for *all* concentrations and chain lengths. This is in accord with very recent experiments [20], but theoretically not well understood. The response of the PE conformation to density changes is much larger in the poor-solvent case [6, 8] than in the good-solvent case [14], and the chain extension behaves non-monotonically as a function of density [6, 8]. Furthermore, in the density regime between $\rho_m\sigma^3 = 10^{-2}$ and 10^{-4} the chain extension and the number of pearls vary most, and almost all monomers are located within the pearls. Upon approaching the dense regime, the string length tends to zero and we find a chain of touching pearls, indicating that the conventional necklace picture breaks down. Our result is compatible with scaling exponents found in scattering experiments [21–23].

Scaling theories [24, 25] have predicted a $\rho_m^{1/2}$-regime to start at ρ_0^*, which is defined at the density where $R_E \approx \xi$, and to extend until $\xi \approx r_{pp}$ where a bead-controlled $\rho_m^{1/3}$-regime starts. We find $\rho_0^*\sigma^3 \simeq 5 \times 10^{-2}, 10^{-3}, 10^{-4}$ for $N_m = 100, 200, 300$, and r_{pp} is equal to ξ between $\rho_m\sigma^3 = 10^{-2}$ and 10^{-1}, so accordingly the $\rho_m^{1/2}$-regime should be visible. One probable reason for our different findings is that the strong inter-chain coupling and the influence of

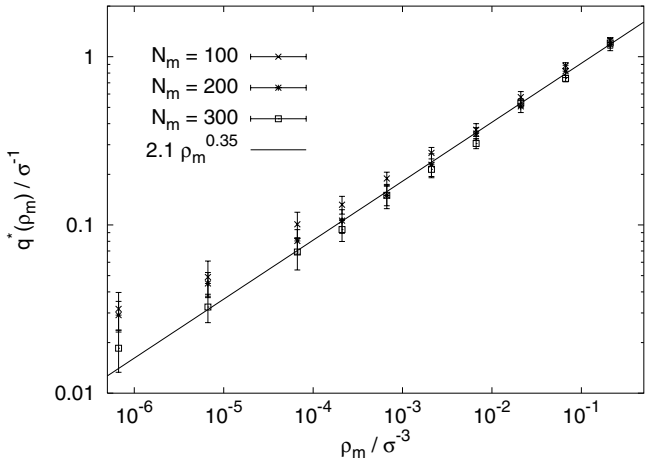

Figure 4. The density dependence of the peak q^* in the structure factor for three different chain lengths $N_m = 100, 200, 300$ with $f = 0.5$ and $\ell_b = 1.5\,\sigma$. The black line is a fit to the data with $N_m = 200$.

the counterions on the conformations are not sufficiently taken into account in the mean-field scaling approach. It is not clear at this stage whether the $\rho_m^{1/2}$-regime can be recovered for much longer chain length. In addition, we observe that the chains form a transient physical network at $\rho_m\sigma^3 = 0.2$ for $N_m \geqslant 200$ which has neither been seen in previous simulations nor predicted by theoretical approaches but is in accord with experimental studies [21–23]. During the simulation these networks reconstruct several times, e.g. chains are not trapped.

A more detailed account of the material presented will be published in forthcoming publications [26, 27].

Acknowledgments

We thank B Dünweg, B Mergell, H Schiessel and M Tamashiro for many fruitful discussions and comments. We gratefully acknowledge partial funding by the DFG SPP 1009 and through the 'Zentrum für Multifunktionelle Werkstoffe und Miniaturisierte Funktionseinheiten', grant BMBF 03N 6500.

References

[1] Hara M (ed) 1993 *Polyelectrolytes: Science and Technology* (New York: Dekker)
[2] Holm C, Kékicheff P and Podgornik R (ed) 2001 *Electrostatic Effects in Soft Matter and Biophysics (NATO Science Series II: Mathematics, Physics and Chemistry, vol 46)* (Dordrecht: Kluwer)
[3] Kantor Y and Kardar M 1994 *Europhys. Lett.* **27** 643
[4] Kantor Y and Kardar M 1995 *Phys. Rev.* E **51** 1299
[5] Dobrynin A V, Rubinstein M and Obukhov S P 1996 *Macromolecules* **29** 2974
[6] Micka U, Holm C and Kremer K 1999 *Langmuir* **15** 4033
[7] Limbach H J and Holm C 2001 *J. Chem. Phys.* **114** 9674
[8] Limbach H J 2001 *PhD Thesis* Johannes Gutenberg Universität, Mainz, Germany
[9] Limbach H J and Holm C 2002 *Comput. Phys. Commun.* **147** 321
[10] Deserno M, Holm C and May S 2000 *Macromolecules* **33** 199
[11] Schiessel H and Pincus P 1998 *Macromolecules* **31** 7953
[12] Khokhlov A 1980 *J. Phys. A: Math. Gen.* **13** 979

[13] Vilgis T A, Johner A and Joanny J-F 2000 *Eur. Phys. J.* E **2** 289
[14] Stevens M J and Kremer K 1995 *J. Chem. Phys.* **103** 1669
[15] Khan M, Mel'nikov S and Jönsson B 1999 *Macromolecules* **32** 8836
[16] Tamashiro M N and Schiessel H 2000 *Macromolecules* **33** 5263
[17] Lyulin A V, Dünweg B, Borisov O V and Darinskii A A 1999 *Macromolecules* **32** 3264
[18] Nierlich M *et al* 1979 *J. Physique* **40** 701
[19] Joanny J F 2001 *Electrostatic Effects in Soft Matter and Biophysics (NATO Science Series II: Mathematics, Physics and Chemistry, vol 46)* ed C Holm, P Kékicheff and R Podgornik (Dordrecht: Kluwer) pp 149–70
[20] Baigl D and Williams C E 2002 at press
[21] Essafi W, Lafuma F and Williams C E 1995 *J. Physique* II **5** 1269
[22] Heitz C, Rawiso M and François J 1999 *Polymer* **40** 1637
[23] Waigh T A, Ober R, Williams C E and Galin J-C 2001 *Macromolecules* **34** 1973
[24] Dobrynin A V and Rubinstein M 1999 *Macromolecules* **32** 915
[25] Dobrynin A V and Rubinstein M 2001 *Macromolecules* **34** 1964
[26] Limbach H J, Holm C and Kremer K 2002 *Europhys. Lett.* **60** at press
(Limbach H J, Holm C and Kremer K 2002 *Preprint* cond-mat/0206274)
[27] Limbach H J and Holm C 2002 at press